

Thermal Goldstino production with low reheating temperaturesAngelo Monteux^{*} and Chang Sub Shin[†]*New High Energy Theory Center, Department of Physics and Astronomy, Rutgers University,
Piscataway, New Jersey 08854, USA*

(Received 18 May 2015; published 4 August 2015)

We discuss thermal production of (pseudo) Goldstinos, the Goldstone fermions emerging from (multiple) SUSY-breaking sectors, when the reheating temperature is well below the superpartner masses. In such a case, the production during the matter-dominated era induced by the inflaton decay stage is more important than after reheating. Depending on the SUSY-breaking scale, Goldstinos are produced by a freeze-in or freeze-out mechanism via $1 \rightarrow 2$ decays and inverse decays. We solve the Boltzmann equation for the momentum distribution function of the Goldstino. In the freeze-out case, Goldstinos maintain chemical equilibrium far after they are kinetically decoupled by elastic scatterings and, consequently, Goldstinos with different momentum decouple at different temperatures. As a result, their momentum distribution function shows a peculiar shape, and the final yield is smaller than if kinetic equilibrium were assumed. We revisit the cosmological implications in both R -parity-conserving and R -parity-violating supersymmetric scenarios. For the former, thermally produced Goldstinos can still be abundant enough to be dark matter at present times even if the reheating temperature is low, of order 1 GeV. For the latter, if the reheating temperature is low, of order 0.1–1 GeV, they are safe from the BBN constraints.

DOI: [10.1103/PhysRevD.92.035002](https://doi.org/10.1103/PhysRevD.92.035002)

PACS numbers: 12.60.Jv, 98.80.Cq, 04.65.+e

I. INTRODUCTION

When considering the consequences of early universe cosmology, it is customary to assume that all interesting phenomena, such as dark matter production, take place after the inflationary period, and in particular after reheating, which marks the moment when the energy density of the inflaton decay products (radiation) dominate over the inflaton energy density. This is justifiable, as any primordial abundance was inflated away and large amounts of entropy are injected during the inflaton decay stage, further diluting any other particle produced during reheating.

However, if the reheating temperature T_R , the maximum temperature of the thermal bath in the radiation-dominated era, is well below the mass scale relevant for the particle production, the abundance produced during the inflaton decay stage could be more important than the one produced after reheating. There are several early works to calculate the production of WIMP-like particles and its phenomenological consequences during this period when the reheating temperature is low enough [1–3]. In this case, the inflaton decay stage can be approximated as the matter-dominated era with constantly injected radiation, and the thermal production can be calculated independently from the specific inflation model. The higher temperature can be achieved during this era and naive (Boltzmann) exponential suppression for the abundance is replaced by power suppression. On the other hand, in the studies of thermal production of super-weakly interacting particles (SWIMP),

e.g. gravitinos and axions, such consideration has been ignored so far, with many works focusing on the production at high T_R .¹

One well-motivated class of SWIMP is a Goldstone- or Goldstino-like particle, ζ , whose interaction to the visible sector is suppressed by the symmetry-breaking scale, and this scale is much higher than its mass. This class of particles is particularly interesting in the sense that their elastic scattering rate is doubly suppressed by the symmetry-breaking scale compared to their production rate. Therefore, the momentum transfer between Goldstinos is only maintained by chemical interactions (inelastic scattering). Actually, this does not give any difference if the production happens at high T_R or during the radiation-dominated era, because chemical interactions also give a thermal distribution for ζ as $f_\zeta(p) \propto e^{-p/T}$. However, if T_R is well below the relevant particle's mass that produces ζ , and the production during the early matter-dominated era is important, the situation is different. As we will show below, the production rate at low temperature is quite momentum dependent, and $f_\zeta(p)$ is no longer proportional to the thermal distribution. Their inverse decay rate becomes more complicated, so a detailed treatment of Boltzmann equations is needed especially when the symmetry-breaking scale is small such as in low-scale gauge mediation.

¹Reference [4] studied the production of gravitinos taking into account a proper treatment of the reheating process, with $T_R \gg \tilde{m}$. In [5], the axino freeze-in thermal production from the neutralino decays is shortly discussed for low reheating temperature after thermal inflation.

^{*}amonteux@physics.rutgers.edu
[†]changsub@physics.rutgers.edu

In this article, we study thermal production of SWIMPs at low reheating temperature considering all the aspects above. We will focus on the production of the Goldstino in supersymmetric theories, but our treatment would apply equally to similar particles. In theories where local supersymmetry (SUSY) is broken spontaneously, the resulting Goldstino is incorporated in the spin-1/2 degrees of freedom of the gravitino, which acquires a mass $m_{3/2} = F/\sqrt{3}M_P$, with F being the scale of SUSY breaking and $M_P = (8\pi G_N)^{-1/2} = 2.4 \times 10^{18}$ GeV, the reduced Planck mass. Because the coupling between the Goldstino and the visible sector is suppressed by $1/F$, their mass and thermal production rate are tightly related. The relation between the Goldstino mass and the interaction strength can be changed if there are multiple sectors with independent SUSY-breaking interactions: multiple Goldstini [6] arise and the scenario deserves more phenomenological interest. In particular, while one Goldstino is still eaten by the gravitino, there are uneaten Goldstini, whose mass is not unambiguously set: at first, in Ref. [6,7], it was shown that they generally acquire a mass $2m_{3/2}$ from supergravity interactions. This was extended in Ref. [8], where it was computed that the Goldstino mass could vary around $2m_{3/2}$ depending on the SUSY-breaking dynamics, and in Ref. [9], where it was shown that, even in the global SUSY limit, the uneaten Goldstinos could receive a large mass (up to $\mathcal{O}(100)$ GeV) if multiple SUSY-breaking sectors communicate with the Standard Model (SM) via gauge interactions. In this last case, the SM fields take the role of messenger fields in mediating SUSY breaking between the two sectors, and large masses for the Goldstino can be achieved. The main interesting change to the standard prediction is that the mass of the uneaten Goldstinos can be parametrically larger than the gravitino mass and can be taken as a free parameter depending on the specifics of the SUSY-breaking dynamics.

This article is structured as follows: in Sec. II, we recall and discuss in more detail the Goldstino interactions. In Sec. III, we discuss the early matter-dominated era and study the production of Goldstinos when the reheating temperature is well below the superpartner scale, $T_R \lesssim \tilde{m}/10$. If the F term is small, the Goldstino is in thermal equilibrium with the MSSM sector during the matter-dominated era and the freeze-out temperature is momentum dependent. This happens because the $2 \rightarrow 2$ scattering that would bring the Goldstinos in kinetic equilibrium has already frozen out, and only the high-momentum Goldstinos can efficiently inverse-scatter into the MSSM thermal bath. We numerically solve the Boltzmann equation for the momentum distribution function (instead of the equation for the number density) and find an analytical solution that reproduces well the numerical results. We compute the resulting Goldstino number yield $Y_\zeta = n_\zeta/s$, which is reduced with respect to the results that one finds assuming kinetic equilibrium.

Otherwise, for a large F term, the Goldstino is slowly produced via superpartner decays (freeze-in). We also consider nonthermal production from direct inflaton decays. We continue in Sec. IV, where we consider the late-time implications of the produced Goldstinos. If R parity is conserved, they can be cold dark matter for reheating temperatures of order 1 GeV, and overclose the Universe for larger T_R ; on the other hand, with R parity violation (RPV) they can decay and will typically interfere with big bang nucleosynthesis (BBN). We derive bounds on the reheating temperature in the range of 0.5–10 GeV for given RPV couplings and Goldstino masses. We present final remarks and conclude in Sec. V.

II. GOLDSTINI INTERACTIONS

If there is a single SUSY-breaking sector, then the corresponding massless fermionic degree of freedom, the Goldstino, forms the spin-1/2 degrees of freedom of the gravitino, which has a mass $m_{3/2} = F/\sqrt{3}M_P$. The situation becomes more complicated if there are multiple sectors with independent SUSY-breaking dynamics [6]: then, in the limit in which each sector is decoupled from the others, each enjoys its own SUSY algebra and, if SUSY breaking occurs independently in each sector, multiple massless Goldstinos would arise. Introducing gravitational interactions, the multiple SUSY algebras are broken down to a diagonal subgroup, and only a linear combination of those Goldstini is eaten by the gravitino. As discussed above, the mass of the uneaten Goldstinos is not proportional to the value of the corresponding F terms and can be taken as a free parameter. For example, consider the case of two SUSY-breaking sectors with hierarchical F terms $F_1 \gg F_2$. The gravitino mass is

$$m_{3/2} = \frac{\sqrt{F_1^2 + F_2^2}}{\sqrt{3}M_P} \approx \frac{F_1}{\sqrt{3}M_P}, \quad (1)$$

while the different Goldstini interactions are suppressed by the different F terms. If each sector contributes SUSY-breaking scalar mass squares $\tilde{m}_{\phi_{1,2}}^2$ and gaugino masses $\tilde{m}_{\lambda_{1,2}}$, we have the following coupling to a matter multiplet (ϕ^i, ψ^i) and gauge multiplet (λ^a, A^a) :

$$\begin{aligned} \mathcal{L}_{\text{int}} \approx & \frac{\tilde{m}_{\phi_1}^2}{F_{\text{eff}}} \eta \psi^i \phi_i^\dagger - \frac{i\tilde{m}_{\lambda_1}}{\sqrt{2}F_{\text{eff}}} \eta \sigma^{\mu\nu} \lambda^a F_{\mu\nu}^a + \frac{\tilde{m}_{\phi_2}^2}{F_\zeta} \zeta \psi^i \phi_i^\dagger \\ & - \frac{i\tilde{m}_{\lambda_2}}{\sqrt{2}F_\zeta} \zeta \sigma^{\mu\nu} \lambda^a F_{\mu\nu}^a + \text{H.c.} \end{aligned} \quad (2)$$

Here we have denoted by η the longitudinal component of the gravitino (the eaten Goldstino) and by ζ the uneaten Goldstino. $F_{\text{eff}} = \sqrt{F_1^2 + F_2^2} \approx F_1$ and $F_\zeta \approx F_2$ are the corresponding F terms of η and ζ , respectively. When $|\tilde{m}_1| \lesssim |\tilde{m}_2|$, the interactions of ζ are enhanced with respect

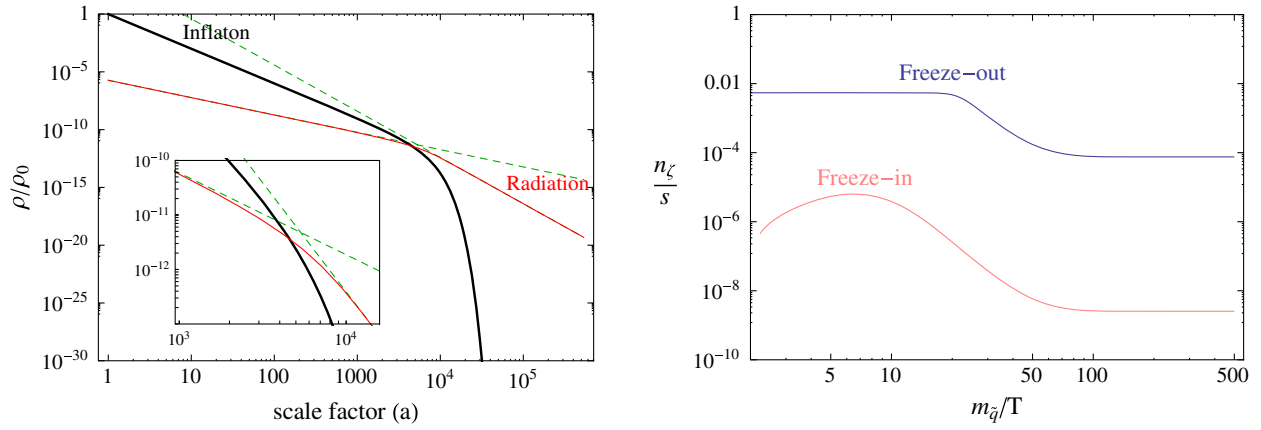


FIG. 1 (color online). Left: Schematic behavior of the energy densities of the inflaton and of thermal radiation (MSSM fields) during the matter-dominated era; as $\rho_r \sim T^4$, we have $T_{\text{MAX}} \gg T_R$. Right: Evolution of the Goldstino yield with fixed reheating temperature $T_R = 20$ GeV (corresponding to $a_R = 5430$), squark mass $m_{\tilde{q}} = 1$ TeV and two choices of $F_\zeta = (100 \text{ TeV})^2$, $(5000 \text{ TeV})^2$, corresponding to freeze-out and freeze-in, respectively.

to those of η , while the mass of ζ can be kept as a free parameter, much greater than F_2/M_P .

In the following, we will focus on the uneaten Goldstino ζ , and we will simply refer to it as the Goldstino. We will denote its F term by F_ζ . It is understood that the spectrum also includes the gravitino, which can be neglected because of its suppressed interactions.

When the temperature falls well below the sparticle mass scale, \tilde{m} , the effective interactions between the Goldstino and other light particles are useful to estimate (nonresonant) elastic scattering rates. After integrating out sparticles, two-Goldstino interactions are given as [10–15]

$$\mathcal{L}_{\text{eff}} = \frac{1}{F_\zeta^2} \bar{\zeta} \bar{\psi}^i \square \zeta \psi_i - \frac{i}{2F_\zeta^2} \zeta \sigma^\mu \partial_\nu \bar{\zeta} F^{a\rho\nu} F_{\mu\rho}^a. \quad (3)$$

If R -parity violating interactions are introduced in the superpotential as $W = \lambda_{ijk} \Phi_i \Phi_j \Phi_k$, there are single-Goldstino interactions even after integrating out sfermions [16],

$$\mathcal{L}_{\text{eff}}^{\text{RPV}} = \sum_{ijk} \frac{1}{\tilde{m}_{\phi_k}^2 F_\zeta} \lambda_{ijk} \psi_i \psi_j \square (\zeta \psi_k) + \text{H.c.} \quad (4)$$

This interaction is not only important to determine the lifetime of the Goldstino, but also to calculate thermal production at low temperatures.

III. GOLDSTINO PRODUCTION IN THE MATTER-DOMINATED ERA

A. Cosmology during reheating

The reheating temperature is usually referred to as the temperature of the thermal bath when the inflaton

decays,² and it is usually defined as $H(T_R) = \Gamma_I$, assuming that the radiation energy density, ρ_r , dominates the Universe. In fact, at the corresponding time $t(T_R) = 1/\Gamma_I$, where Γ_I is the decay rate of the inflaton, the inflaton energy density is still non-negligible and a temperature defined in this way was achieved only during matter domination. Thus, entropy injection is still occurring after T_R . One more precise way to define T_R is to consider the asymptotic behaviors of ρ_r in both matter- and radiation-dominated epochs, as shown in Fig. 1,

$$\begin{aligned} \rho_r &= \frac{\pi^2 g_*(T)}{30} T^4 \\ &= \begin{cases} (\pi^2 g_*(T) T_R^4 / 30) (a/a_R)^{-3/2} & \text{for } T \gg T_R, \\ (\pi^2 g_*(T) T_R^4 / 30) (a/a_R)^{-4} & \text{for } T \ll T_R, \end{cases} \end{aligned} \quad (5)$$

where $g_*(T)$ is the effective number of massless degrees of freedom at the temperature T , a is the scale factor and a_R is the scale at which two asymptotic lines meet. Numerically we get

$$T_R = 0.7 \left(\frac{90}{\pi^2 g_*(T_R)} \right)^{1/4} \sqrt{\Gamma_I M_P}. \quad (6)$$

This will be our definition of the reheating temperature.

On the other hand, the thermal bath in the matter-dominated era reached a higher temperature,

²While we will be referring to the inflaton as the field dominating the energy density of the Universe in the early matter-dominated era, there are other cases that reproduce the same scaling of the energy density, $\rho_X \sim a^{-3}$; a typical example would be the late decay of moduli, which typically result in very low reheating temperatures. In any case, we will refer to the reheating temperature as the maximum temperature achieved in the last radiation-dominated era, the one leading to big bang nucleosynthesis.

$$T_{\text{MAX}} = \left(\frac{24g_*(T_R)}{5\pi^2 g_*^2(T_{\text{MAX}})} \right)^{1/8} \left(\frac{\mu}{T_R} \right)^{1/2} T_R, \quad (7)$$

where $\mu = V_I^{1/4}$ is the energy scale of inflation, and slow-roll was assumed for this simplified expression. Because of the continuous entropy injection during the matter-dominated period, the temperature scales as $T/T_{\text{MAX}} \propto a^{-3/8}$ instead of the typical scaling of the radiation-dominated era, $T \propto a^{-1}$ (see Fig. 1). We refer to Ref. [2] for the details of the computations leading to T_{MAX} . It is sufficient here to note that $T_{\text{MAX}} \gg T_R$ can be much larger than the TeV (sparticle mass) scale, for typical inflation scales $\mu \sim 10^8 \text{ GeV} - 10^{16} \text{ GeV}$. The hierarchy of relevant scales can be summarized as

$$m_\psi, m_\zeta, T_R \ll \tilde{m} = \mathcal{O}(\text{TeV}) \lesssim T_{\text{MAX}}, \quad (8)$$

where ψ are SM particles, m_ζ is the mass of ζ , which is taken as the NLSP by assuming $m_{3/2} < m_\zeta \ll \tilde{m}$. We consider the thermal production of Goldstinos at $T \lesssim T_{\text{MAX}}$, when T_R is taken low, $T_R = \mathcal{O}(\text{GeV})$.

The Goldstino can be produced (and annihilated) via three different channels: (i) scattering: $\phi + A_\mu \leftrightarrow \zeta + \psi, \lambda + \lambda \leftrightarrow \zeta + \lambda, \dots$, (ii) (inverse) decay: $\phi \leftrightarrow \zeta + \psi, \lambda \leftrightarrow \zeta + A_\mu, \dots$, and (iii) RPV scattering: $\psi + \psi \leftrightarrow \zeta + \psi$ (here $\psi, \phi, \lambda, A_\mu$, respectively, stand for SM fermions, sfermions, gauginos, and gauge bosons).

The Boltzmann equation for the number density n_ζ can be written as

$$\begin{aligned} \dot{n}_\zeta + 3Hn_\zeta = & g_\zeta \int \frac{d^3 \mathbf{p}_\zeta}{(2\pi)^3} C[f_\zeta] \\ = & \langle \sigma_{\phi A_\mu \rightarrow \zeta \psi} v \rangle_{\phi A_\mu} n_\phi n_{A_\mu} - \langle \sigma_{\zeta \psi \rightarrow \phi A_\mu} v \rangle_{\zeta \psi} n_\zeta n_\psi + \dots \quad (\text{i}) \\ + & \langle \Gamma_{\phi \rightarrow \zeta \psi} \gamma^{-1} \rangle_\phi n_\phi - \langle \sigma_{\zeta \psi \rightarrow \phi} v \rangle_{\zeta \psi} n_\zeta n_\psi + \dots \quad (\text{ii}) \\ + & \langle \sigma_{\psi \psi \rightarrow \zeta \psi} v \rangle_{\psi \psi} n_\psi n_\psi - \langle \sigma_{\zeta \psi \rightarrow \psi \psi} v \rangle_{\zeta \psi} n_\zeta n_\psi, \quad (\text{iii}) \end{aligned} \quad (9)$$

where $\gamma = 1/\sqrt{1-v^2}$, $n_{\psi_i} \equiv g_{\psi_i} \int d^3 \mathbf{p}_i / (2\pi)^3 f_{\psi_i}(\mathbf{p}_i)$ and

$$\begin{aligned} \langle \mathcal{O} \rangle_{\psi_i \dots \psi_j} & \equiv \frac{1}{n_{\psi_i} \dots n_{\psi_j}} \\ & \times \int \frac{g_{\psi_i} d^3 \mathbf{p}_i}{(2\pi)^3} \dots \frac{g_{\psi_j} d^3 \mathbf{p}_j}{(2\pi)^3} f_{\psi_i}(\mathbf{p}_i) \dots f_{\psi_j}(\mathbf{p}_j) \mathcal{O}. \end{aligned} \quad (10)$$

Here, $\Gamma_{\phi \rightarrow \zeta \psi}$ is defined in the rest frame. We take $n_\Psi = n_\Psi^{\text{eq}}$ for $\Psi = \phi, \psi, \lambda, A_\mu$ because they are all in thermal equilibrium for the relevant temperature scale. One might rewrite the inverse scattering and decay terms in the rhs of the Boltzmann equation, and Eq. (9) becomes

$$\begin{aligned} \dot{n}_\zeta + 3Hn_\zeta = & \langle \sigma_{\phi A_\mu \rightarrow \zeta \psi} v \rangle_T n_\phi^{\text{eq}} n_{A_\mu}^{\text{eq}} \\ & + \langle \Gamma_{\phi \rightarrow \zeta \psi} \gamma^{-1} \rangle_T n_\phi^{\text{eq}} + \dots (1 - n_\zeta/n_\zeta^{\text{eq}}) \\ \equiv & \Gamma_{\text{prod}}^\zeta (n_\zeta^{\text{eq}} - n_\zeta), \end{aligned} \quad (11)$$

where $\langle \dots \rangle_T$ denotes thermal average. In the treatment of the Boltzmann equation, we have neglected quantum-statistical effects (Pauli-blocking/Bose-enhancement), as we have $f_i \lesssim 1$. For the low F term, these (Goldstino-number-changing) interactions can be in chemical equilibrium at high temperatures, until the interaction rate drops below the Hubble rate and the process freezes out. The production rate $\Gamma_{\text{prod}}^\zeta$ of Eq. (11) determines the chemical freeze-out (decoupling) temperature, $T_{\text{f.o.}}$, defined by $3H(T_{\text{f.o.}}) = \Gamma_{\text{prod}}^\zeta$. Depending on the value of $T_{\text{f.o.}}$, two distinct situations for the Goldstino production are possible, displayed in Fig. 1:

- (i) freeze-in: for $T_{\text{f.o.}} \gg \tilde{m}$, Goldstino interactions were not in thermal equilibrium when superpartners were abundant; Goldstino abundance is gradually increased to a maximum, after which they are diluted.
- (ii) freeze-out: for $T_{\text{f.o.}} \ll \tilde{m}$, Goldstinos maintain chemical equilibrium with the superpartners until the latter are not abundant.

Since the production at high temperatures $T \gtrsim \tilde{m}$ is diluted away, we can only focus on the production for $T \lesssim \tilde{m}$. At such low temperature, the Boltzmann equation can be much simplified by ignoring the scattering contribution to the production of ζ [17,18]; for $T_{\text{f.o.}} \gg \tilde{m}$, the freeze-in production by $\phi \rightarrow \zeta + \psi$ ($\lambda \rightarrow \zeta + A_\mu$) dominates over the diluted freeze-out contribution. One can also neglect the inverse decay term given by $n_\zeta/n_\zeta^{\text{eq}}$ in the last expression of the second line of Eq. (11).

For the freeze-out case, the situation is more subtle. It should be noted that the factorization by $(1 - n_\zeta/n_\zeta^{\text{eq}})$ leading to Eq. (11) is only valid if ζ is in kinetic equilibrium, or at least if $f_\zeta(\mathbf{p}')/f_\zeta(\mathbf{p}) = e^{-(p'-p)/T}$. It is possible for the Goldstino to elastically scatter off of the thermal bath as given by the interactions in Eq. (3): if the elastic interaction rate is large enough, the Goldstinos would be in kinetic equilibrium with the thermal bath. However, because the $\zeta + \psi(A_\mu) \rightarrow \zeta + \psi(A_\mu)$ process is suppressed by F_ζ^2 while the single-Goldstino production channels are suppressed only by F_ζ , kinetic decoupling takes place before chemical decoupling.³ To be precise, the momentum distribution of ζ is determined not only by elastic scattering but also by chemical interactions. Thus, if the production happens at $T \gg \tilde{m}$, energy-momentum conservation just tells us that the momentum distribution

³This is the opposite behavior from the WIMPs. Even after chemical decoupling, WIMPs elastically scatter off of the thermal bath and remain in kinetic equilibrium until lower temperatures.

of thermally produced ζ would be the form of $f_\zeta(\mathbf{p}) \propto e^{-p/T}$. Also if the chemical interactions are efficient enough (thus, for small F_ζ), the produced Goldstinos will still have a equilibrium distribution function, $f_\zeta(\mathbf{p}) = f_\zeta^{\text{eq}} = \exp(-p/T)$. These arguments are not sufficient to justify the form of equation around the time of decoupling, since as we will see, at low T with small F_ζ term, Goldstinos with different momentum decouple at different temperatures and, in the absence of elastic scattering, do not rethermalize. Furthermore, the continuous entropy injection during the matter-dominated era causes the Goldstinos decoupled earlier to be colder than those decoupled later. Therefore, it is necessary to solve the nonintegrated version of the Boltzmann equation for the distribution function $f_\zeta(\mathbf{p})$:

$$\frac{df_\zeta}{dt} = \frac{\partial f_\zeta}{\partial t} - H p \frac{\partial f_\zeta}{\partial p} = C[f_\zeta]. \quad (12)$$

Substituting $H dt = d \ln a$, for $T \lesssim \tilde{m}$ this can be rewritten as

$$\begin{aligned} \frac{\partial f_\zeta}{\partial \ln a} - \frac{\partial f_\zeta}{\partial \ln p} &= \left(1 - \frac{f_\zeta}{e^{-p/T}}\right) \left(\frac{\Gamma_{\phi \rightarrow \zeta \psi} \tilde{m}_\phi T}{H p^2}\right) \\ &\times \exp\left\{-\frac{p}{T} \left(1 + \frac{\tilde{m}_\phi^2}{4p^2}\right)\right\} \\ &+ (\phi \rightarrow \lambda, \psi \rightarrow A_\mu) \end{aligned} \quad (13)$$

in the limit of $m_\zeta \rightarrow 0$. In the Appendix, we provide the Boltzmann equation for non-negligible $m_\zeta \lesssim \tilde{m}$. In the following, we will only consider decays from one generation of squarks, \tilde{q} , with mass $m_{\tilde{q}}$ of $\mathcal{O}(\text{TeV})$, while the others are assumed to be heavier. Adding other contributions is straightforward. For example, production by gaugino decays will take the same form with the substitution $m_{\tilde{q}} \rightarrow m_{\tilde{g}}$ and changing the number of sfermions to number of gauginos. For simplicity, the number of massless degrees of freedom $g_*(T)$ is taken constant, $g_* = 85$, in the whole range $T_R \lesssim T \lesssim m_{\tilde{q}}$.

The freeze-out temperature for $T_{\text{f.o.}} \lesssim m_{\tilde{q}}$ is calculated from

$$\begin{aligned} 3H(T_{\text{f.o.}}) &= 1.4 \left(\frac{5\pi^2 g_*}{72}\right)^{1/2} \frac{T_{\text{f.o.}}^4}{M_P T_R^2} \\ &= \sum_{\text{l gen}} \langle \Gamma_{\tilde{q} \rightarrow \zeta q} \gamma^{-1} \rangle_T n_{\tilde{q}}^{\text{eq}} / n_\zeta^{\text{eq}} \\ &\simeq \frac{12 m_{\tilde{q}}^5}{16 \pi F_\zeta^2} \sqrt{\pi} \left(\frac{m_{\tilde{q}}}{T_{\text{f.o.}}}\right)^{3/2} e^{-m_{\tilde{q}}/T_{\text{f.o.}}}, \end{aligned} \quad (14)$$

where $\Gamma_{\tilde{q} \rightarrow \zeta q} = m_{\tilde{q}}^5 / (16 \pi F_\zeta^2)$, and the result is

$$T_{\text{f.o.}} = \frac{m_{\tilde{q}}}{21.2 + \delta}, \quad (15)$$

with $\delta = 5.5 \ln \frac{m_{\tilde{q}}}{20 T_{\text{f.o.}}} + \ln \frac{m_{\tilde{q}}}{\text{TeV}} + 2 \ln \frac{(100 \text{ TeV})^2}{F_\zeta} + \frac{1}{2} \ln \frac{85}{g_*} + 2 \ln \frac{T_R}{10 \text{ GeV}}$.

This value is no longer true for a large F term. In this case, the freeze-out temperature becomes well above $m_{\tilde{q}}$, and it is mostly determined by the scattering process. The freeze-out abundance is quite diluted by entropy production, and freeze-in production dominates the Goldstino abundance as shown in Fig. 1.

In the following, we derive the Goldstino yield for each case of freeze-in and -out.

B. Freeze-in

First, we will consider the simpler case of intermediate or high F_ζ , for which Goldstinos never reach chemical equilibrium for $T \lesssim m_{\tilde{q}}$; their abundance is gradually increased by the thermal decay process until it is not efficient, after which they are diluted during the rest of the matter-dominated era.

For $n_\zeta \ll n_\zeta^{\text{eq}}$, the resulting yield at reheating can be computed as

$$\begin{aligned} \left(\frac{n_\zeta}{s}\right)_{\text{FI}} &= \frac{1}{s_R} \int_{t_i}^{t_R} dt \left(\frac{a}{a_R}\right)^3 \sum_{\text{l gen}} \langle \Gamma_{\tilde{q} \rightarrow \zeta q} \gamma^{-1} \rangle n_{\tilde{q}}^{\text{eq}} \\ &= \frac{15.6 M_P \sum_{\text{l gen}} \Gamma_{\tilde{q} \rightarrow \zeta q}}{g_*^{3/2} T_R^5} \int_{T_R}^{T_{\text{f.o.}}} \frac{dT}{T} \left(\frac{T}{T}\right)^{12} \\ &\times \frac{K_1(m_{\tilde{q}}/T)}{K_2(m_{\tilde{q}}/T)} n_{\tilde{q}}^{\text{eq}} \\ &\simeq 2 \times 10^{-7} \left(\frac{85}{g_*}\right)^{3/2} \left(\frac{T_R}{10 \text{ GeV}}\right)^7 \\ &\times \left(\frac{(500 \text{ TeV})^2}{F_\zeta}\right)^2 \left(\frac{\text{TeV}}{m_{\tilde{q}}}\right)^4, \end{aligned} \quad (16)$$

where $s_R \equiv (2\pi^2 g_*/45) T_R^3$, and t_R is the time at $a = a_R$. K_α is the modified Bessel function of the second kind, and $K_1(x)/K_2(x) \simeq 1-3/(2x)$ for $x \gg 1$. t_i is the initial time and we took it at the freeze-out of chemical interactions. The integrand on the second line shows high powers of (T_R/T) caused by entropy injection and temperature dependence of the freeze-in production rate, and because the Boltzmann suppression factor at low T from $n_{\tilde{q}}^{\text{eq}}$, the production rate is most efficient around $T \simeq m_{\tilde{q}}/10$. The final result in Eq. (16) is obtained assuming $T_R \ll m_{\tilde{q}}/10 \ll T_{\text{f.o.}}$. Given the expression (15) for $T_{\text{f.o.}}$, this corresponds to $F_\zeta \gg (500 \text{ TeV})^2$ for $m_{\tilde{q}} = 1 \text{ TeV}$. For lower values of F_ζ , the freeze-out abundance is more important, which will be treated next. Here we just note that this yield is sizable and we will discuss late-time implications in Sec. IV.

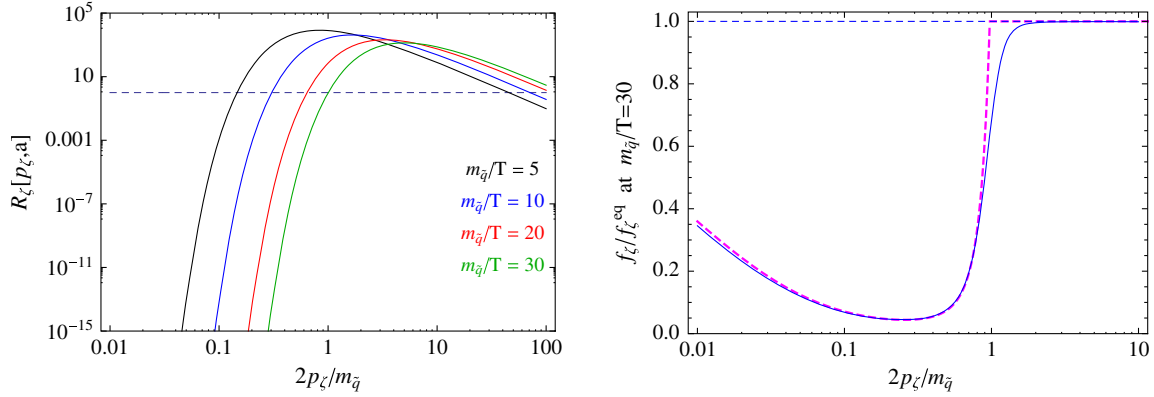


FIG. 2 (color online). Left: Effective ratio between the production rate and the Hubble parameter, as a function of the Goldstino momentum and for different temperatures. Interactions are in chemical equilibrium when $R_\zeta \gg 1$, while the low-momentum region is frozen-out. Right: Ratio between the Goldstino distribution function and the equilibrium distribution function, at $m_{\bar{q}}/T = 30$. The continuous line comes from the numerical integration of the Boltzmann equation, while the magenta dashed line is the approximate analytical solution of Eq. (22).

C. Freeze-out

For smaller F_ζ , one could solve the same Boltzmann equation, (9)–(11), and find

$$\left(\frac{n_\zeta}{s}\right)_{\text{FO}}^{\text{eq}} = 1.7 \times 10^{-6} \left(\frac{85}{g_*}\right) \left(\frac{T_R}{10 \text{ GeV}}\right)^5 \left(\frac{50 \text{ GeV}}{T_{\text{f.o.}}}\right)^5. \quad (17)$$

This would be incorrect, because the rhs of the Boltzmann equation (11) was found assuming that the Goldstinos are in kinetic equilibrium with the rest of the thermal bath. When Goldstinos are injected in the bath via decays of nonrelativistic particles, their momentum distribution is peaked around $m_{\bar{q}}/2$. Because the $2 \rightarrow 2$ elastic scattering is frozen out at a higher temperature, it does not thermalize the distribution function. The result is that Goldstinos with high momentum easily inverse decay back into superpartners, while Goldstinos at low momentum are effectively frozen out. Therefore, one can expect the correct value would be smaller than Eq. (17).

This behavior can be understood explicitly by looking at the rhs of the Boltzmann equation for the distribution function, Eq. (13). We can estimate the effective ratio between the production rate and the expansion rate as

$$R_\zeta(p, a) \equiv \sum_{\text{I gen}} \frac{\Gamma_{\bar{q} \rightarrow \zeta q} m_{\bar{q}} T^2}{H p^3} \exp\left(-\frac{m_{\bar{q}}^2}{4Tp}\right). \quad (18)$$

For a given scale factor a (corresponding to a given temperature $T(a)$), $R_\zeta(p, a)$ changes with the momentum;

in particular, if $R_\zeta(p, a) \ll 1$, the Goldstinos with momentum p are decoupled, while if $R_\zeta(p, a) \gg 1$ they are in equilibrium. In Fig. 2, we plot R_ζ as a function of p for different temperatures, fixing $m_{\bar{q}} = 1 \text{ TeV}$, $F_\zeta = (100 \text{ TeV})^2$, $T_R = 20 \text{ GeV}$. For example, at $T = m_{\bar{q}}/5 = 200 \text{ GeV}$ all Goldstinos with momentum $p \gtrsim 50 \text{ GeV}$ are in thermal equilibrium, while at $T = m_{\bar{q}}/10 = 100 \text{ GeV}$ only the Goldstinos with momentum $p \gtrsim 150 \text{ GeV} = 1.5T$ are, with the Goldstino whose momentum is smaller than the temperature all decoupled. Thus at $T \approx m_{\bar{q}}/10$ the result is an earlier departure of the number density from its equilibrium value compared to that of assuming kinetic equilibrium, Eq. (15) (this earlier departure can also be seen in Fig. 6 in the Appendix).

Because R_ζ becomes very small once it is below one, we can solve the Boltzmann equation with zero rhs at low momentum,

$$\frac{df_\zeta(p, a)}{d \ln a} - \frac{df_\zeta(p, a)}{d \ln p} = 0 \quad \text{for } p < p_{\text{f.o.}}(a), \quad (19)$$

with boundary condition $f_\zeta(p, a) = e^{-p/T(a)}$ for $p \geq p_{\text{f.o.}}(a)$. Here $p_{\text{f.o.}}(a)$ is the freeze-out momentum at a given temperature $T(a)$, defined by $R_\zeta(p_{\text{f.o.}}(a), a) = 1$:

$$p_{\text{f.o.}}(a) = \frac{(k_\zeta m_{\bar{q}})^2}{T(a)}, \quad (20)$$

$$\kappa_\zeta = 0.13 \left(\frac{62.3}{62.3 + 4 \ln \frac{T}{50 \text{ GeV}} + 8 \ln \frac{(100 \text{ TeV})^2}{F_\zeta} + 2 \ln \frac{85}{g_*} + 8 \ln \frac{T_R}{20 \text{ GeV}} + 24 \ln \frac{0.13}{\kappa_\zeta}} \right)^{1/2}. \quad (21)$$

Finally, the solution to the Boltzmann equation is

$$f_\zeta(p, a) = \begin{cases} \exp[-(p/T_\zeta(a))^{6/11}], & p < p_{\text{f.o.}}(a) \\ \exp[-p/T(a)], & p > p_{\text{f.o.}}(a) \end{cases} \quad (22)$$

$$T_\zeta(a) = \left(\frac{T_R}{\kappa_\zeta m_{\tilde{q}}} \right)^{5/3} \left(\frac{a_R T_R}{a} \right). \quad (23)$$

To illustrate this better, in Fig. 2 we show the ratio between the resulting Goldstino distribution function and the equilibrium distribution function, $f_\zeta \propto e^{-p/T}$, for a given temperature $T = m_{\tilde{q}}/30 \approx 33$ GeV. In blue, we show the results from numerical integration of the Boltzmann equation; in dashed, the analytical expression for the distribution function, Eq. (22), is shown, in good agreement with the numerical results. It is seen that the Goldstinos at high momentum are in equilibrium, while the low-momentum ones are suppressed.

The late-time yield at low temperatures $T \lesssim T_R$, is given by

$$\left(\frac{n_\zeta}{s} \right)_{\text{FO}} = 6.8 \times 10^{-7} \left(\frac{85}{g_*} \right) \left(\frac{T_R}{10 \text{ GeV}} \right)^5 \left(\frac{130 \text{ GeV}}{\kappa_\zeta m_{\tilde{q}}} \right)^5. \quad (24)$$

This is shown in Fig. 3, where we also show the result following from the kinetic equilibrium assumption, Eq. (17), and the abundance found without considering the matter-dominated epoch (that is, the case $T_R = T_{\text{MAX}}$) in which the Boltzmann suppression of the superpartner number density results in a negligible Goldstino abundance at low reheating temperatures. Comparing the blue and magenta lines, we can conclude that a naive treatment of the

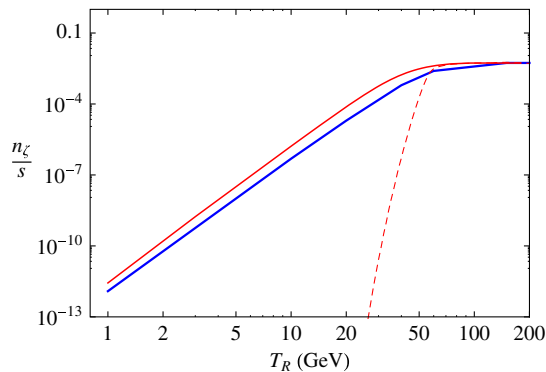


FIG. 3 (color online). Late-time Goldstino yield as a function of the reheating temperature T_R , given $F_\zeta = (100 \text{ TeV})^2$ and $m_{\tilde{q}} = 1 \text{ TeV}$. The blue line represents the numerical results, which coincide with the analytical result of Eq. (24), while the red line is the result that one would have found if kinetic equilibrium was assumed. The dashed red line is the yield found neglecting the matter-dominated era.

Boltzmann equation overestimates the abundance by a factor of about 3.

As a reminder, these results were found in the limit of small m_ζ , but they do not change much if the Goldstino mass is sizeable. Even for $m_\zeta = 100$ GeV, the final yield changes only by about 10%. In the Appendix, we show the full Boltzmann equation for the massive case, as well as numerical results for m_ζ up to 200 GeV (see Fig. 6).

Finally, as the distribution function deviates from the kinetic equilibrium case, one can also consider if the Goldstinos produced would form colder or warmer dark matter, when compared to the case in which the particles are in kinetic equilibrium. The average momentum for the Goldstino at $T \lesssim T_R$ can be evaluated as

$$\langle p \rangle \approx 26T_\zeta(a) = 0.36T \left(\frac{g_*(T)}{g_*} \right)^{1/3} \left(\frac{T_R}{10 \text{ GeV}} \right)^{5/3} \times \left(\frac{130 \text{ GeV}}{\kappa_\zeta m_{\tilde{q}}} \right)^{5/3}. \quad (25)$$

This should be compared to the thermal averaged value $\langle p \rangle_T \approx 3T$. For low reheating temperatures, Goldstinos are colder than the background temperature. This is due to two competing effects: at first, they are produced at a higher momentum, $p \approx m_{\tilde{q}}/2$, after which they are redshifted between production and reheating. For low T_R , the second effect is dominant.

D. Nonthermal production

Goldstinos can also be produced nonthermally, for example by direct moduli/inflaton decays, or by squark (or other lightest WIMP particles in the MSSM) decays after freeze-out, for which $n_\zeta/s = n_{\tilde{q}}/s$. The former is a model-dependent effect and it can be sizable or not. Concerning the latter, it can be important for large F terms: first of all, the lifetime of the squark (with $m_{\tilde{q}} = 1 \text{ TeV}$) has to be short enough to decay before BBN, implying $F_\zeta \lesssim (10^5 \text{ TeV})^2$ [6]. Then, if $F_\zeta \gtrsim (5 \times 10^4 \text{ TeV})^2$, the lifetime of squark is long enough to decay after squark freeze-out by pair annihilation. In this case, the resulting energy density of the Goldstinos is given by the nonthermal contribution,

$$\Omega_\zeta h^2 = \frac{m_\zeta}{m_{\tilde{q}}} \Omega_{\tilde{q}} h^2. \quad (26)$$

Since the reheating temperature is lower than the freeze-out temperature of squark annihilation, $T_{fr}^{\tilde{q}\tilde{q}^*}$, $\Omega_{\tilde{q}} h^2$ is also diluted by a factor of $(T_R/T_{fr}^{\tilde{q}\tilde{q}^*})^3$ compared to usual freeze-out abundance with $T_R \rightarrow \infty$ [2]. Because of the substantial model-dependence in the nonthermal Goldstino abundance, the results in Eqs. (16)–(24) should be considered as conservative results, as it is always possible to

produce more Goldstinos by introducing nonthermal processes.

IV. LATE-TIME IMPLICATIONS

The Goldstinos produced in the early matter-dominated era are generally lighter than any other superpartner, except the gravitino. As such, they can provide a metastable dark matter candidate, even for very low reheating temperatures, $T_R \sim 1$ GeV. The lifetime for the decay to a gravitino, $\zeta \rightarrow \psi_{3/2} \psi_{SM} \bar{\psi}_{SM}$ was computed in Ref. [6] as

$$\tau_\zeta \approx 10^{22} \text{ sec} \left(\frac{F_\zeta}{(100 \text{ TeV})^2} \right)^2 \left(\frac{100 \text{ GeV}}{m_\zeta} \right)^7. \quad (27)$$

Although this is typically larger than the age of the Universe, $t_0 \approx 10^{17}$ sec, indirect detection limits on decaying dark matter are more stringent, with lower limits $\tau_{\text{DM}} \gtrsim \mathcal{O}(10^{26}-10^{27})$ sec for dark matter decaying to quark-antiquark pairs [19–21]. As a crude estimate, we take the same order of magnitude, $\tau_\zeta^{\text{min}} \approx 10^{26}$ sec for the limits on the decaying Goldstino. These can be avoided with Goldstini lighter than 100 GeV, or larger F_ζ .

A. Assuming R parity

If R parity is conserved, the Goldstino is effectively stable in most of the parameter space. For a small F term (corresponding to Goldstinos produced before freeze-out), the present dark matter density is

$$(\Omega_\zeta h^2)_{\text{FO}} = 0.19 \left(\frac{m_\zeta}{1 \text{ MeV}} \right) \left(\frac{85}{g_*} \right) \left(\frac{T_R}{10 \text{ GeV}} \right)^5 \left(\frac{130 \text{ GeV}}{k_\zeta m_{\bar{q}}} \right)^5. \quad (28)$$

The allowed region is shown in Fig. 4, and spans the range $0.5 \text{ GeV} \lesssim T_R \lesssim 30 \text{ GeV}$. The result is only logarithmically dependent on the increase of F_ζ , until $F_\zeta = (500 \text{ TeV})^2$, for which $T_{\text{f.o.}} > m_{\bar{q}}/10$. For a larger F term, the relevant process is freeze-in, and the dark matter abundance can be evaluated from Eq. (16):

$$(\Omega_\zeta h^2)_{\text{FI}} = 0.11 \left(\frac{m_\zeta}{2 \text{ MeV}} \right) \left(\frac{85}{g_*} \right)^{3/2} \left(\frac{T_R}{10 \text{ GeV}} \right)^7 \times \left(\frac{(500 \text{ TeV})^2}{F_\zeta} \right)^2 \left(\frac{1 \text{ TeV}}{m_{\bar{q}}} \right)^4. \quad (29)$$

To summarize this section, the observed dark matter abundance can easily be produced in a matter-dominated era, at temperatures above a low reheating temperature T_R .

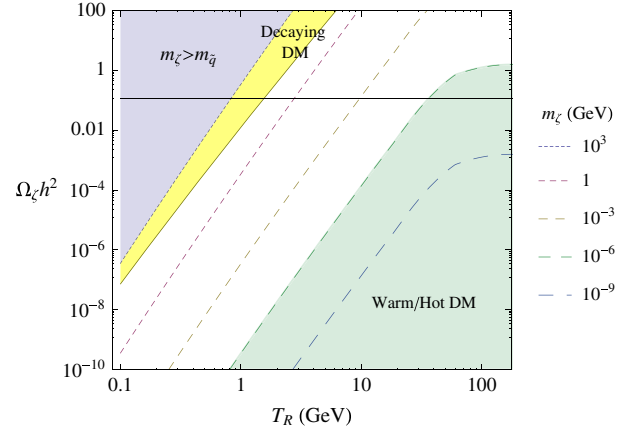


FIG. 4 (color online). Late-time energy density of Goldstinos, with a small F term $F_\zeta = (100 \text{ TeV})^2$ and $m_{\bar{q}} = 1 \text{ TeV}$, for different values of the Goldstino mass. For $m_\zeta < 1 \text{ keV}$ the Goldstino is warm or hot dark matter. For m_ζ in the range $100 \text{ GeV} - 1 \text{ TeV}$ (yellow region) the Goldstino lifetime, Eq. (27), is too short, $\tau \lesssim 10^{26}$ sec, and is excluded by DM indirect detection constraints. The horizontal black line marks the observed value of the DM abundance, $\Omega_{\text{DM}} h^2 = 0.12$.

B. Assuming R -parity violation

Another well-motivated possibility is that of R -parity violation. In the general case, baryon and lepton number would be violated and the proton would be unstable. Nevertheless, if lepton or baryon number were to be independently conserved on their own, proton stability would be achieved accidentally. In the following, we will discuss the case in which baryon number is violated while lepton number is conserved (the other case will have a similar phenomenology). This is also interesting because baryonic R -parity violation can account for the matter-antimatter asymmetry of the Universe with low reheating temperatures, while other scenarios (such as leptogenesis) require higher temperatures. The baryonic RPV operator in the superpotential is

$$W_{\text{BRPV}} = \frac{\lambda''_{ijk}}{2} u_i^c d_j^c d_k^c + \text{H.c.}, \quad (30)$$

where the contraction of the color indices with an ϵ^{abc} tensor is understood, and as a consequence, $j \neq k$.

In low-scale gauge mediation with a single SUSY-breaking sector, the gravitino is very light and there are still proton decay channels of the type $p \rightarrow K \psi_{3/2}$, mediated by RPV interactions. The resulting limits are very stringent and were discussed in [22,23]. In the case of multiple Goldstini, the proton could potentially decay to any Goldstino lighter than 1 GeV. This is particularly dangerous when F_ζ is small, independently of the Goldstino mass: for example, the weakest limit is

$$|\lambda''_{323}| < 1.31 \times 10^{-6} \left(\frac{m_{\bar{q}}}{1 \text{ TeV}} \right)^2 \frac{F_{\zeta}}{(100 \text{ TeV})^2}. \quad (31)$$

To avoid this constraint, we require that $m_{\zeta} > m_p$; however, now it is the Goldstino which is unstable, as the decay channel $\zeta \rightarrow u_i d_j d_k$ is open. The lifetime is

$$\tau_{\zeta} = 1.57 \times 10^3 \text{ sec} \left(\frac{1}{|\lambda''_{ijk}|} \right)^2 \left(\frac{10 \text{ GeV}}{m_{\zeta}} \right)^9 \left(\frac{m_{\bar{q}}}{1 \text{ TeV}} \right)^4 \times \left(\frac{F_{\zeta}}{(100 \text{ TeV})^2} \right)^2, \quad (32)$$

where $|\lambda''_{ijk}|$ is the largest RPV coupling for which the decay is kinematically accessible. As the Goldstino mass naturally lies in the interval 1–100 GeV, the top quark is not accessible and the most relevant operator with few constraints from flavor physics is $\lambda''_{223} c^c b^c s^c$ [24].

The lifetime (32) of the Goldstino naturally falls in a range that is probed by big bang nucleosynthesis: if a large amount of energy is injected during the thermal plasma during BBN, the primordial abundance of light elements is changed and would go against observations. In particular, the case of hadronic decays was studied in great details in Refs. [25–28]. In the following, we will use the results of Ref. [26], where limits on the abundance $M_X Y_X$ of a decaying particle X were set in the lifetime range $10^{-2} \text{ sec} < \tau_X < 10^{12} \text{ sec}$, for different masses $M_X = 100 \text{ GeV}, 1 \text{ TeV}, 10 \text{ TeV}$.

As we are also interested in particles with lighter masses, we need to extrapolate their results to $M_X = 10 \text{ GeV}$ and below. Therefore, we will shortly review the source of the limits. For short lifetimes ($\tau < 10^2 \text{ sec}$), the mesons and nucleons produced by X thermalize quickly, and the main

consequence of the decay is the increase of the neutron-to-proton ratio, n/p , resulting in larger abundances of D and ${}^4\text{He}$. For longer lifetimes, mesons decay and primary protons and neutrons scatter inelastically off of the background nuclei, generating hadronic showers, dissociating ${}^4\text{He}$ and producing D, T, ${}^3\text{He}$, which also result in higher amounts of ${}^6\text{Li}$, ${}^7\text{Li}$. At $\tau > 10^7 \text{ sec}$, the neutrons decay away and only protons are left, with a smaller effect on ${}^4\text{He}$ -dissociation. On the other hand, electromagnetic decay products (γ, e^+, e^-) are thermalized by processes such as $\gamma + \gamma_{\text{BG}} \rightarrow e^+ + e^-$ if their energy is above the threshold $E_{\text{th}} = m_e^2/22T$ [29]; one should compare this threshold to the binding energy of D and ${}^4\text{He}$, respectively, 2.2 and 28.3 MeV: if it is higher, nonthermalized photons will dissociate deuterium and helium. As the bath temperature decreases with time, photo-dissociation of D and ${}^4\text{He}$ is active for $\tau > 10^4 \text{ sec}$ and $\tau > 10^6 \text{ sec}$, respectively.

We simulate the Goldstino decay with PYTHIA 8.2 [30] and get the total number of charged particles and EM energy per ζ decay, for different values of m_{ζ} . We then translate the results of Ref. [26] to lower masses. For the sake of simplicity, we only use the dominant constraints [that is, primordial helium abundance (Y_p), deuterium to hydrogen ratio (D/H) and helium-4 to deuterium ratio (${}^4\text{He}/\text{D}$)]. Our results are shown in Fig. 5, where for comparison we also show the constraints of Ref. [26].

For most of the lifetime range, the limits on $m_{\zeta} Y_{\zeta}$ are of order 10^{-12} – 10^{-14} GeV . Comparing this to the yields found in Eqs. (16) and (24), only very low reheating temperatures are allowed. In Fig. 5, we show contours of the maximum allowed reheating temperatures in the $m_{\zeta} - \lambda''_{ijk}$ plane: apart from a small shaded region in the top right corner, for which $\tau_{\zeta} < 10^{-2} \text{ sec}$, the upper limit on the reheating temperature

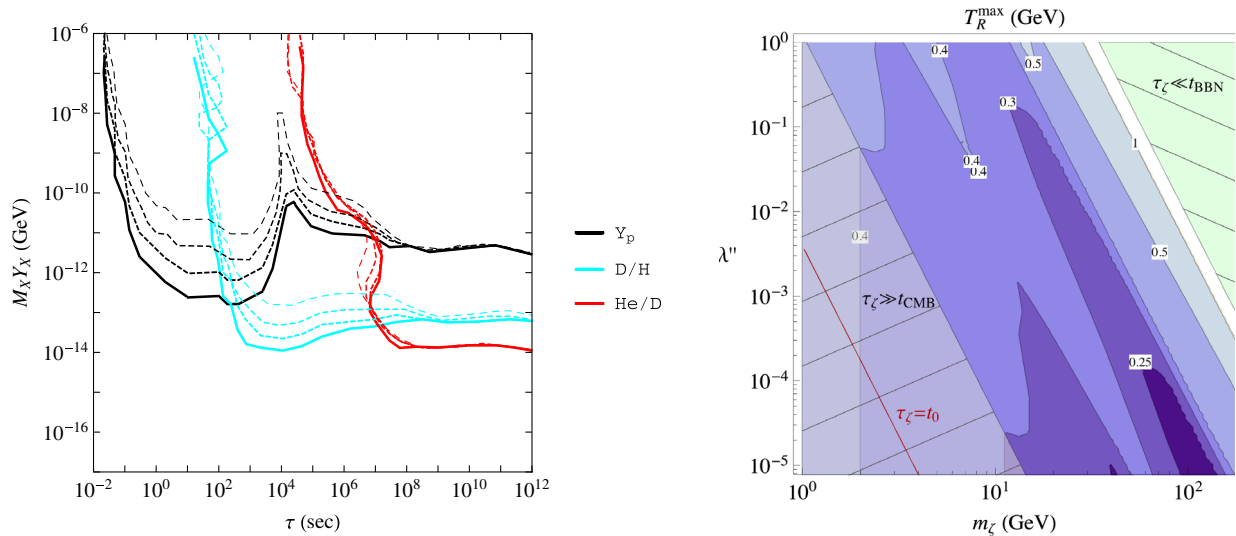


FIG. 5 (color online). Left: Upper limits on the energy density of a hadronically decaying particle X , with, from bottom to top, $M_X = 10 \text{ GeV}, 100 \text{ GeV}, 1 \text{ TeV}, 10 \text{ TeV}$, evaluated from Ref. [26]. Right: Maximum reheating temperature allowed by BBN constraints while varying λ''_{ijk} and m_{ζ} . The other parameters are fixed as $F_{\zeta} = (100 \text{ TeV})^2$ and $m_{\bar{q}} = 1 \text{ TeV}$.

is of order 0.5 GeV. In the lower left corner, we shaded the area in which $\tau_\zeta \gg 10^{12}$ sec and Goldstino decays do not interfere with BBN: here they would be constrained by diffuse x-ray and γ -ray emissions, and the limits on $m_\zeta Y_\zeta$ are typically more strict than the BBN ones. As this discussion is beyond the scope of the present paper, we only display the BBN limits as a conservative bound.

In the presence of R -parity violation, there is one more channel for the production of Goldstini that had not been analyzed so far in the literature: the scattering $qq \rightarrow q\zeta$ does not require any on-shell superpartners, in contrast with the R -parity conserving processes discussed above. Using the interaction in Eq. (4), the freeze-out temperature for the scattering is

$$T_{\text{f.o.}}^{\text{RPV}} = 70 \text{ GeV} \left(\frac{g_*}{85}\right)^{1/10} \left(\frac{F_\zeta}{(100 \text{ TeV})^2}\right)^{2/5} \left(\frac{m_{\tilde{q}}}{\text{TeV}}\right)^{4/5} \times \left(\frac{1}{\lambda''}\right)^{2/5} \left(\frac{10 \text{ GeV}}{T_R}\right)^{2/5}. \quad (33)$$

The Goldstino distribution is the same as that in kinetic equilibrium as long as they are in chemical equilibrium, and once we solve the relevant Boltzmann equation we find the yield,

$$\begin{aligned} \left(\frac{n_\zeta}{s}\right)_{\text{RPV}} &= 7.0 \times 10^{-7} |\lambda''|^2 \ln \frac{T_{\text{f.o.}}^{\text{RPV}}}{T_R} \left(\frac{85}{g_*}\right)^{3/2} \left(\frac{T_R}{10 \text{ GeV}}\right)^7 \\ &\times \left(\frac{(100 \text{ TeV})^2}{F_\zeta}\right)^2 \left(\frac{\text{TeV}}{m_{\tilde{q}}}\right)^4 \\ &+ 4.7 \times 10^{-8} |\lambda''|^2 \left(\frac{85}{g_*}\right)^{3/2} \left(\frac{T_R}{10 \text{ GeV}}\right)^7 \\ &\times \left(\frac{(100 \text{ TeV})^2}{F_\zeta}\right)^2 \left(\frac{\text{TeV}}{m_{\tilde{q}}}\right)^4. \end{aligned} \quad (34)$$

Here the first term of RHS shows the production during the matter-dominated era and the second term is the production after reheating; in general, the former dominates over the latter, and the R -parity conserving freeze-out contribution from Eq. (24) is larger than both. For the RPV production rate to be sizable, the only option would be $T_R = T_{\text{MAX}} \ll \tilde{m}$, for which there is no early matter-dominated era. In this case, only the last term in the equation above contributes to Goldstino production. There are still strong limits from BBN, and the maximum reheating temperature is of order 1–10 GeV, with smaller RPV couplings allowing slightly larger reheating temperatures ($T_R^{\text{max}} \approx 20 \text{ GeV}$ for $\lambda'' = 10^{-5}$).

The limits on the reheating temperature cited so far corresponded to $F_\zeta = (100 \text{ TeV})^2$, with Goldstinos generated at freeze-out. The dependence of T_R^{max} on larger F terms is first logarithmic, until $F_\zeta \approx (500 \text{ TeV})^2$, and then scales as $T_R^{\text{max}} \propto (F_\zeta / (500 \text{ TeV})^2)^{2/7}$ when the freeze-in

contribution (16) becomes dominant. For example, $F_\zeta = (10^6 \text{ TeV})^2$ corresponds to $T_R^{\text{max}} \approx 100 \text{ GeV}$ for $m_\zeta = 10 \text{ GeV}$ and $\lambda''_{ijk} = 1$.

We end this section by summarizing the strong bounds on the reheating temperature in the case in which R parity is violated. For the freeze-out case, the maximum reheating temperature allowed by BBN constraints is of order 1 GeV.

Some implications for what concerns baryogenesis can be drawn: because any baryon asymmetry produced at higher temperatures in the matter-dominated era will be diluted away, the baryon asymmetry should be generated at temperatures between T_R and $T_{\text{BBN}} \sim 10 \text{ MeV}$. This is possible in the LSP baryogenesis scenario of Ref. [31] if the Goldstino decays before BBN (in the upper right corner of Fig. 5): for example, with parameters chosen as $F_\zeta = (100 \text{ TeV})^2$, $\lambda''_{ijk} \approx 0.1$, the Goldstino abundance in Eq. (24) can be large enough for baryogenesis if $m_\zeta \approx T_R \approx 50 \text{ GeV}$.

Even though we have taken $m_{\tilde{q}} = 1 \text{ TeV}$ as a benchmark point, it is worth noting that current LHC limits on RPV squarks are less stringent: for a light top squark decaying to three quarks, the CMS Collaboration excludes masses up to 350–385 GeV in Ref. [32]. Gluino limits are stronger: in Ref. [33], CMS excludes gluinos in the decay channel $\tilde{g} \rightarrow tbs$ up to 900 GeV, while in the same channel ATLAS excludes gluinos up to 874 GeV, with limits of order 800 GeV for different flavor composition of the final states. Thus, squarks are still allowed to be lighter than in our benchmark point.

V. CONCLUSIONS

In this work, we have discussed thermal production of Goldstinos as an example of super-weakly interacting particles during an early matter-dominated era ending at reheating. This is important when the reheating temperature is low, in the GeV range or below, as particle production through an heavier sector (superparticles) occurs only at higher temperatures that were not achieved during radiation domination.

We have analyzed in detail the production of an uneaten Goldstino by solving the Boltzmann equation for its momentum distribution function and revisited the cosmological implications. When the Goldstino is stable enough, thermal production can provide the correct dark matter density even for reheating temperatures as small as 1 GeV. If R parity is violated, the Goldstino has to be heavier than the proton and is metastable, with a lifetime range that naturally interferes with BBN. In this case, reheating temperatures higher than 1 GeV are excluded for almost all of the small F_ζ parameter space.

Such low reheating temperatures suggest a low scale of inflation and/or introducing certain symmetries to prevent coupling between the inflaton and visible fields. For example, if the inflaton decay rate to the MSSM is Planck suppressed, $\Gamma_I = m_I^3 / M_P^2$, the reheating temperature

is $T_R \simeq 1 \text{ GeV}(m_I/10^3 \text{ TeV})^{3/2}$. In this case we can also find an upper bound on T_{MAX} from its definition in Eq. (7), $T_{\text{MAX}} \lesssim 10^3 \text{ TeV}(T_R/\text{GeV})^{2/3}$. Since the nonthermal production is proportional to $T_R/m_I \propto T_R^{1/3}$, it could be more important at low reheating temperature, and full analysis considering a specific inflation model is needed. In this paper, we presented thermal production of Goldstino as model independent contributions. Our results are conservative bounds on the abundance, because the non-thermal productions of SWIMP are just additive quantities.

We showed that the Goldstino is one of many good examples in which a momentum dependent process gives a sizable difference compared to that assuming thermal distribution of the momentum, even if they are produced from thermal bath. Such effects are also discussed in Ref. [34] for the production of sterile neutrino dark matter, and in Ref. [35] for leptogenesis from heavy Majorana neutrino decays. Since the period of kinetic decoupling and production mechanism are also important to the evolution of density perturbation of dark matter, the study of the full Boltzmann equations in the perturbed spacetime can give observable consequences for small scale structures.

ACKNOWLEDGMENTS

We would like to thank Matt Buckley, David Shih, Scott Thomas and Stefano Profumo for useful discussions about this subject. A. M. and C. S. S. are supported in part by DOE Grants No. DOE-SC0010008, No. DOE-ARRA-SC0003883, and No. DOE-DE-SC0007897.

APPENDIX: BOLTZMANN EQUATION FOR MASSIVE GOLDSTINO

In this section we derive the Boltzmann equation for the momentum distribution function of ζ , $f_\zeta(\mathbf{p})$, keeping the dependence on a nonzero mass m_ζ . The dominant source of production is sfermion decays, $\phi \rightarrow \zeta + \psi$, when the temperature is lower than the sfermion mass \tilde{m}_ϕ , and the contribution from elastic scattering is ignored. As we did in the rest of this work, we will consider the Boltzmann equation and distribution functions in the classical limit, i.e. assuming $f_\chi(\mathbf{p}) \lesssim 1$, and $f_\chi^{\text{eq}}(\mathbf{p}) \simeq e^{-E_\chi/T}$, where $E_\chi = \sqrt{m_\chi^2 + \mathbf{p}^2}$ for particle χ . The corresponding Boltzmann equation in the limit of massless quarks is

$$\begin{aligned} \frac{df_\zeta}{dt} &= \frac{\partial f_\zeta}{\partial t} - H p \frac{\partial f_\zeta}{\partial p} = C[f_\zeta] \\ &= \frac{g_\phi g_\psi}{2E_\zeta} \int \frac{d^3 \mathbf{p}_\phi}{(2\pi)^3 2E_\phi} \frac{d^3 \mathbf{p}_\psi}{(2\pi)^3 2p_\psi} \\ &\quad \times (2\pi)^4 \delta^{(4)}(p_\phi^\mu - p_\psi^\mu - p^\mu) |\mathcal{M}_{\phi \rightarrow \zeta \psi}|^2 (f_\phi - f_\zeta f_\psi), \end{aligned} \quad (\text{A1})$$

where $p = |\mathbf{p}|$. Tree level T symmetry ensures $|\mathcal{M}_{\phi \rightarrow \zeta \psi}|^2 = |\mathcal{M}_{\zeta \psi \rightarrow \phi}|^2$ at leading order. Sfermions are in thermal equilibrium, which is maintained by the interactions with the background SM fields ($\phi + \phi^* \leftrightarrow A_\mu + A_\mu$, $\phi + \psi \rightarrow \phi + \psi$, ...) before such interactions are frozen. After that, the distribution of sfermions is determined by the interaction with the Goldstinos, and we need to solve the coupled Boltzmann equations. However, most of the Goldstinos are produced before the freeze-out of sfermion-SM interactions, so we can safely take $f_\phi(\mathbf{p}_\phi) = e^{-E_\phi/T}$.

Using the identity $f_\phi^{\text{eq}} \delta^{(4)}(p_\phi^\mu - p_\psi^\mu - p^\mu) = f_\zeta^{\text{eq}} f_\psi^{\text{eq}} \delta^{(4)}(p_\phi^\mu - p_\psi^\mu - p^\mu)$ to represent f_ψ , after integrating over \mathbf{p}_ψ , we get

$$\begin{aligned} C[f_\zeta] &= \left(1 - \frac{f_\zeta}{f_\zeta^{\text{eq}}}\right) \frac{g_\phi g_\psi |\mathcal{M}|^2}{2E_\zeta} \int \frac{dp_\phi}{(8\pi)} f_\phi^{\text{eq}} \frac{p_\phi^2}{E_\phi p_\psi^*} \\ &\quad \times \int d \cos \theta_{\phi\zeta} \delta(E_\phi - E_\zeta - p_\psi^*) \\ &= \left(1 - \frac{f_\zeta}{f_\zeta^{\text{eq}}}\right) \frac{g_\phi g_\psi |\mathcal{M}|^2}{16\pi E_\zeta} \int_{D[p]} dp_\phi \frac{p_\phi^2}{E_\phi p_\psi^*} \\ &\quad \times \frac{e^{-E_\phi/T}}{|dp_\psi^*/d \cos \theta_{\phi\zeta}|}, \end{aligned} \quad (\text{A2})$$

where $p_\psi^* = \sqrt{p_\phi^2 + p^2 - 2p_\phi p \cos \theta_{\phi\zeta}}$, so $|dp_\psi^*/d \cos \theta_{\phi\zeta}| = p_\phi p / p_\psi^*$. For given p , the integral domain $D[p]$ is determined by $E_\phi - E_\zeta = \sqrt{p_\phi^2 + p^2 - 2p_\phi p \cos \theta_{\phi\zeta}}$ for $-1 \leq \cos \theta_{\phi\zeta} \leq 1$. Then, we find $p_\phi^- \leq p_\phi \leq p_\phi^+$, where

$$p_\phi^\mp = m_\phi^2 \frac{(E_\zeta \mp p)}{2m_\zeta^2} - \frac{(E_\zeta \pm p)}{2}. \quad (\text{A3})$$

In terms of energy variable E_ϕ , $E_\phi^- \leq E_\phi \leq E_\phi^+$, where

$$E_\phi^\mp = m_\phi^2 \frac{(E_\zeta \mp p)}{2m_\zeta^2} + \frac{(E_\zeta \pm p)}{2}. \quad (\text{A4})$$

In the massless limit, $m_\zeta \rightarrow 0$, we obtain

$$\frac{m_\phi^2}{4p} + p < E_\phi, \quad (\text{A5})$$

which was used in Eq. (13). It is straightforward to evaluate $C[f_\zeta]$ as

$$\begin{aligned}
 C[f_\zeta] &= \left(1 - \frac{f_\zeta}{f_\zeta^{\text{eq}}}\right) \frac{g_\phi g_q |\mathcal{M}|^2}{16\pi E_\zeta p} \int_{E_\phi^-}^{E_\phi^+} dE_\phi e^{-E_\phi/T} \\
 &= \left(1 - \frac{f_\zeta}{e^{-E_\zeta/T}}\right) \left(\frac{g_\phi \Gamma_{\phi \rightarrow \zeta q} m_\phi T}{g_\zeta E_\zeta p}\right) [e^{-E_\phi^-/T} - e^{-E_\phi^+/T}].
 \end{aligned}
 \tag{A6}$$

Finally, the Boltzmann equation can be written as

$$\begin{aligned}
 \frac{\partial f_\zeta}{\partial \ln a} - \frac{\partial f_\zeta}{\partial \ln p} \\
 = (1 - e^{E_\zeta/T} f_\zeta) \left(\frac{\Gamma_{\phi \rightarrow \zeta q} m_\zeta T}{HE_\zeta p}\right) [e^{-E_\phi^-/T} - e^{-E_\phi^+/T}].
 \end{aligned}
 \tag{A7}$$

This expression replaces Eq. (13) in the case of non-negligible m_ζ .

For example, in Fig. 6 we show the evolution of the Goldstino number density for different values of the Goldstino mass for a fixed $T_R = 40$ GeV. From top to bottom, with the continuous lines we show the yield computed assuming kinetic equilibrium and $m_\zeta = 0$, and the yields computed solving the above Boltzmann equation for three different values of the masses, $m_\zeta = 0, 100, 200$ GeV. We find that the final yield of Goldstinos is not

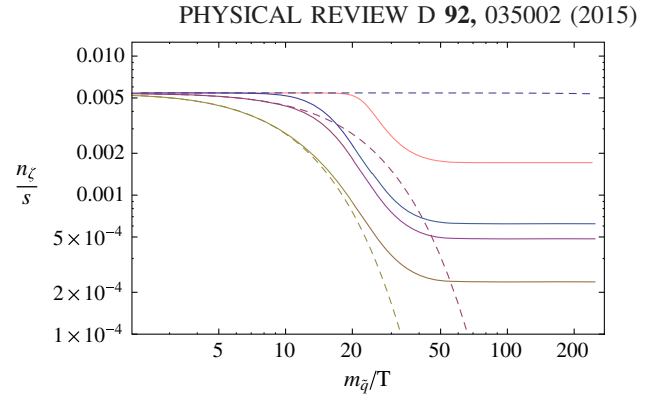


FIG. 6 (color online). Evolution of the Goldstino number density for non-negligible m_ζ . Here we have fixed $m_{\tilde{q}} = 1$ TeV, $F_\zeta = (100 \text{ TeV})^2$ and $T_R = 40$ GeV. From top to bottom, the continuous lines are the yield computed assuming kinetic equilibrium in the massless case, and the yields using the full Boltzmann equation, for three different values of the masses, $m_\zeta = 0, 100, 200$ GeV. The dashed lines are equilibrium number densities for the same masses.

changed much for $m_\zeta \lesssim 100$ GeV. The dashed lines are the equilibrium number densities for the three different masses: we see that the effect of the masses is much smaller than what was naively expected by looking at the equilibrium number density.

-
- [1] D. J. Chung, E. W. Kolb, and A. Riotto, *Phys. Rev. D* **60**, 063504 (1999).
- [2] G. F. Giudice, E. W. Kolb, and A. Riotto, *Phys. Rev. D* **64**, 023508 (2001).
- [3] L. Roszkowski, S. Trojanowski, and K. Turzynski, *J. High Energy Phys.* **11** (2014) 146.
- [4] V. S. Rychkov and A. Strumia, *Phys. Rev. D* **75**, 075011 (2007).
- [5] S. Kim, W.-I. Park, and E. D. Stewart, *J. High Energy Phys.* **01** (2009) 015.
- [6] C. Cheung, Y. Nomura, and J. Thaler, *J. High Energy Phys.* **03** (2010) 073.
- [7] C. Cheung, F. D'Eramo, and J. Thaler, *J. High Energy Phys.* **08** (2011) 115.
- [8] N. Craig, J. March-Russell, and M. McCullough, *J. High Energy Phys.* **10** (2010) 095.
- [9] R. Argurio, Z. Komargodski, and A. Mariotti, *Phys. Rev. Lett.* **107**, 061601 (2011).
- [10] Z. Komargodski and N. Seiberg, *J. High Energy Phys.* **09** (2009) 066.
- [11] A. Brignole, F. Feruglio, and F. Zwirner, *Nucl. Phys.* **B501**, 332 (1997).
- [12] M. A. Luty and E. Ponton, *Phys. Rev. D* **57**, 4167 (1998).
- [13] A. Brignole, F. Feruglio, and F. Zwirner, *J. High Energy Phys.* **11** (1997) 001.
- [14] T. Lee and G.-H. Wu, *Mod. Phys. Lett. A* **13**, 2999 (1998).
- [15] A. Brignole, J. Casas, J. Espinosa, and I. Navarro, *Nucl. Phys.* **B666**, 105 (2003).
- [16] E. Dudas, G. von Gersdorff, D. Ghilencea, S. Lavignac, and J. Parmentier, *Nucl. Phys.* **B855**, 570 (2012).
- [17] L. Covi, L. Roszkowski, and M. Small, *J. High Energy Phys.* **07** (2002) 023.
- [18] C. Cheung, G. Elor, and L. Hall, *Phys. Rev. D* **84**, 115021 (2011).
- [19] G. Bertone, W. Buchmuller, L. Covi, and A. Ibarra, *J. Cosmol. Astropart. Phys.* **11** (2007) 003.
- [20] A. Massari, E. Izaguirre, R. Essig, A. Albert, E. Bloom, and Germán Arturo Gómez-Vargas, *Phys. Rev. D* **91**, 083539 (2015).
- [21] G. Giesen, M. Boudaud, Y. Genolini, V. Poulin, M. Cirelli *et al.*, [arXiv:1504.04276](https://arxiv.org/abs/1504.04276).
- [22] K. Choi, E. J. Chun, and J. S. Lee, *Phys. Rev. D* **55**, R3924 (1997).
- [23] K. Choi, K. Hwang, and J. S. Lee, *Phys. Lett. B* **428**, 129 (1998).
- [24] R. Barbier, C. Berat, M. Besancon, M. Chemtob, A. Deandrea *et al.*, *Phys. Rep.* **420**, 1 (2005).
- [25] M. Kawasaki, K. Kohri, and T. Moroi, *Phys. Lett. B* **625**, 7 (2005).

- [26] M. Kawasaki, K. Kohri, and T. Moroi, *Phys. Rev. D* **71**, 083502 (2005).
- [27] K. Jedamzik, *Phys. Rev. D* **70**, 063524 (2004).
- [28] K. Jedamzik, *Phys. Rev. D* **74**, 103509 (2006).
- [29] M. Kawasaki and T. Moroi, *Prog. Theor. Phys.* **93**, 879 (1995).
- [30] T. Sjöstrand, S. Ask, J. R. Christiansen, R. Corke, N. Desai, P. Ilten, S. Mrenna, S. Prestel, C. O. Rasmussen, and P. Z. Skands, *Comput. Phys. Commun.* **191**, 159 (2015).
- [31] A. Monteux and C. S. Shin, *J. Cosmol. Astropart. Phys.* 05 (2015) 035 .
- [32] V. Khachatryan *et al.* (CMS), *Phys. Lett. B* **747**, 98 (2015).
- [33] S. Chatrchyan *et al.* (CMS), *J. High Energy Phys.* 01 (2014) 163.
- [34] X.-D. Shi and G. M. Fuller, *Phys. Rev. Lett.* **82**, 2832 (1999).
- [35] A. Basboll and S. Hannestad, *J. Cosmol. Astropart. Phys.* 01 (2007) 003.